

An upper bound of the silhouette validation metric for clustering

Hugo Sträng^{a,*}, Tai Dinh^{b,*}

^aIndependent researcher, Stockholm, Sweden

^bThe Kyoto College of Graduate Studies for Informatics, 7 Tanaka Monzencho, Sakyo Ward, Kyoto City, Kyoto, Japan

Abstract

The silhouette coefficient quantifies, for each observation, the balance between within-cluster cohesion and between-cluster separation, taking values in $[-1, 1]$. The average silhouette width (ASW) is a widely used internal measure of clustering quality, with higher values indicating more cohesive and well-separated clusters. However, the dataset-specific maximum of ASW is typically unknown, and the standard upper limit of 1 is rarely attainable. In this work, we derive for each data point a sharp upper bound on its silhouette width and aggregate these to obtain a canonical upper bound on the ASW. This bound—often substantially below 1—enhances the interpretability of empirical ASW values by indicating how close a given clustering result is to the best possible outcome on that dataset. It can be used to confirm global optimality, guide the evaluation of clustering solutions, and be refined to incorporate minimum cluster-size constraints for greater practical relevance. Finally, we extend the framework to establish a corresponding bound for the macro-averaged silhouette.

Keywords: Data mining, cluster analysis, internal evaluation metric, silhouette score, average silhouette width, upper bound

1. Introduction

Cluster analysis is a fundamental tool in data science for discovering structure in unlabeled data (Aggarwal, 2013). Its applications span the natural and social sciences, engineering, education, economics, and the health sciences (Dinh et al., 2025). Because ground-truth labels are rarely available, evaluating clustering quality is challenging, so researchers rely on internal validation indices that summarize within-cluster compactness and between-cluster separation (Jain et al., 1999).

Among the cluster validation indices, the silhouette width (also known as the silhouette coefficient, silhouette score, or silhouette index) is one of the most widely used measures to assess how well each point fits within its assigned cluster relative to its nearest neighboring cluster (Rousseeuw, 1987). The average of this measure across all data points is often referred to as the average silhouette width ASW. ASW values close to 1 signal well-separated, compact clusters; values near 0 imply overlapping clusters; and negative values indicate that points are likely misassigned. Extensive work has examined and refined ASW. Batool & Hennig (2021) proved that it satisfies key axioms for clustering quality measures such as scale invariance and consistency. More recently, Pavlopoulos et al. (2025) examined alternative aggregation strategies that improve ASW’s robustness to cluster-size imbalance.

Although ASW is widely used, its raw values are difficult to interpret across heterogeneous datasets. Intrinsic data characteristics impose strict ceilings on attainable ASW scores; for example, when clusters overlap or deviate from convex shapes,

even the best partition may yield a low ASW. Comparing ASW values across datasets with different properties can therefore lead to misguided conclusions about cluster quality.

To address this issue, we derive a data-dependent upper bound on the ASW. This bound supplies essential context: if analysis shows that no partition can exceed, say, an ASW of 0.30, an empirical result of 0.29 should be regarded as essentially optimal. Such insight prevents wasted effort in pursuit of negligible gains and enables more informed evaluation of clustering quality.

The biggest obstacle in silhouette optimization is the combinatorial explosion of the solution space as the number of samples increases. Even for moderately sized datasets, the number of possible clusterings is astronomical, rendering optimization through exhaustive search with respect to any internal criterion computationally prohibitive. Batool & Hennig (2021) addressed this limitation by proposing two heuristic algorithms that search for local maxima of ASW, noting that global optimization is tractable only for the smallest datasets. Our contribution complements their approach by providing a data-aware benchmark against which the quality of such locally optimal solutions can be evaluated.

The main contributions are as follows:

- We introduce a novel data-dependent upper bound on the ASW, computable in $O(n^2 \log n)$ time, to yield a *global* ceiling that no clustering of the given dissimilarity matrix can surpass.
- We evaluate the proposed upper bound on large-scale synthetic datasets and a diverse suite of real-world datasets across multiple dissimilarity measures. We show that the bound is nearly tight in many of the cases examined.

*Corresponding author: Hugo Sträng (hugo.strang2@gmail.com), Tai Dinh (t_dinh@kgi.edu)

Silhouette coefficient for x_1 :

$$a(x_1) = \frac{d_{12} + d_{13}}{2} \text{ (intra-cluster distance)}$$

$$b(x_1) = \frac{d_{14} + d_{15}}{2} \text{ (inter-cluster distance to the nearest cluster)}$$

$$s(x_1) = \frac{b(x_1) - a(x_1)}{\max(a(x_1), b(x_1))}$$

Average silhouette: mean of $s(x_i)$ for all i

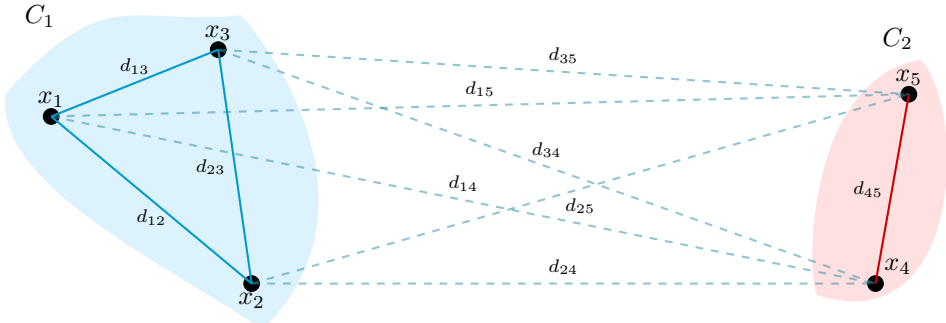


Figure 1: Illustration of the silhouette coefficient calculation.

- All datasets, preprocessing scripts, bound computation routines, and experiment notebooks are publicly released in a GitHub repository¹ and PyPI² to ensure full reproducibility and to encourage further research and practical adoption.

The rest of this paper is organized as follows. Section 2 reviews related works. Section 3 introduces preliminaries. Section 4 details the proposed method. Section 5 presents the experimental results. Finally, section 6 summarizes the findings and outlines directions for future research.

2. Related work

The silhouette coefficient (Rousseeuw, 1987) is a distance-based internal validity index that quantifies how well each object fits into its assigned cluster relative to its nearest alternative. Fig. 1 illustrates the construction. For a point x_i in cluster C_ℓ , we measure within-cluster cohesion by $a(x_i)$ —its average dissimilarity to the other members of C_ℓ —and nearest-cluster separation by $b(x_i)$ —its average dissimilarity to the closest neighboring cluster. These quantities yield an individual silhouette score $s(x_i) \in [-1, 1]$, which is large when separation dominates cohesion, near zero around decision boundaries, and negative when x_i is, on average, closer to another cluster than to its own. Aggregating over points gives the ASW, a dataset-level summary of partition quality.

In practice, ASW is often used for model selection by choosing the number of clusters K that maximizes it. Despite numerous extensions—e.g., to categorical data (Dinh et al., 2019), fuzzy clustering (Lasek et al., 2024), hierarchical clustering (Owoo & Odei-Mensah, 2025), model-based clustering (Guan et al., 2025), spectral clustering (Xian & Liu, 2025), spherical clustering (Deng et al., 2025), and optimization-based methods (Yang et al., 2024)—the original silhouette framework remains a standard baseline for benchmarking clustering algorithms.

Other commonly used internal validation indices include the Davies–Bouldin index (Davies & Bouldin, 1979) and the

Calinski–Harabasz index (Caliński & Harabasz, 1974), which also evaluate compactness and separation but rely on alternative formulations of intra- and inter-cluster dispersion.

In this work, we focus on the silhouette due to its interpretability and widespread adoption across both research and applied domains. To account for cluster-size imbalance, we additionally employ the *macro-averaged* silhouette, defined as the unweighted mean of per-cluster silhouette averages. This variant ensures that smaller clusters contribute equally to the overall assessment, providing a more balanced view of clustering quality.

Silhouette-optimization. PAMSIL (Partitioning Around Medoids based on SILhouette) is a modification of the classical PAM algorithm (Kaufman & Rousseeuw, 1990), designed to directly optimize the ASW (Van der Laan et al., 2003). Unlike K -means or standard K -medoids, which minimize within-cluster dissimilarities, PAMSIL explicitly seeks cluster configurations that maximize ASW. It achieves this by modifying the SWAP phase of PAM: in each iteration, the algorithm performs the swap that yields the largest improvement in ASW and terminates once no further improvement is possible, ensuring convergence to a local optimum. An efficient implementation of PAMSIL is available in the open-source K-Medoids Python package (Schubert & Lenssen, 2022). Moreover, Fatima Batool and Christian Hennig have proposed alternative algorithms that find local ASW optima (Batool & Hennig, 2021).

External validation indices. When ground-truth class labels are available, external validation measures provide a way to quantify how well a clustering agrees with a known reference partition. Two of the most commonly used indices are the adjusted Rand index (ARI) (Hubert & Arabie, 1985) and the adjusted mutual information (AMI) (Vinh et al., 2009). Both adjust their underlying similarity measures for chance agreement, ensuring that random labelings yield expected scores near zero.

The ARI extends the classical Rand index by comparing all pairs of samples and counting how consistently they are assigned to the same or different clusters in both partitions. Its normalization accounts for random overlap, producing values in $[-1, 1]$ with 1 indicating identical partitions. The AMI applies a similar correction to the mutual information (MI) between

¹<https://github.com/hugo-strang/silhouette-upper-bound>

²<https://pypi.org/project/silhouette-upper-bound/>

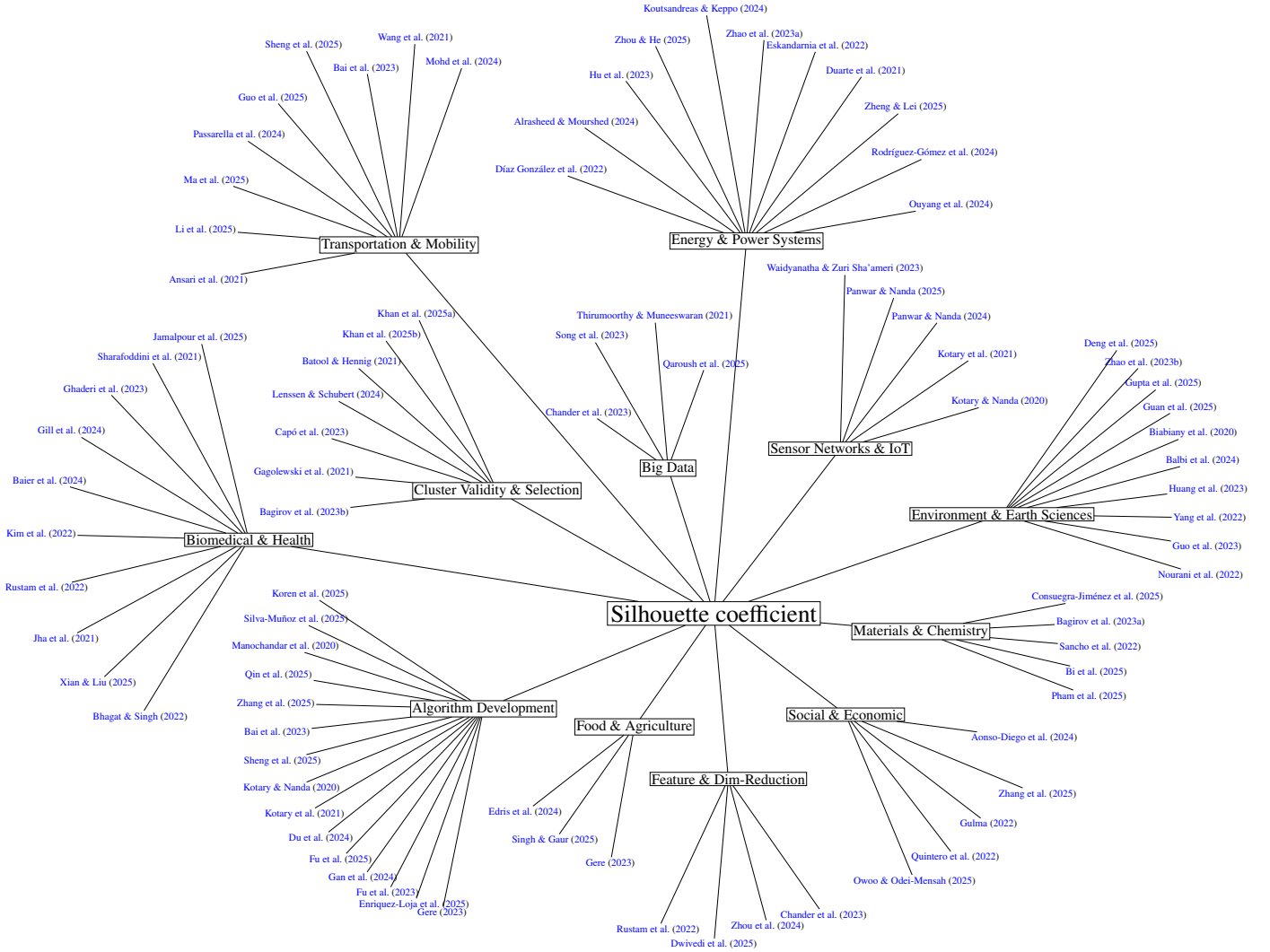


Figure 2: Taxonomy of how the silhouette coefficient is employed across research fields.

partitions, normalizing it by the expected MI under random assignments and bounding the result between 0 and 1.

Both indices are symmetric, easy to interpret, and widely used in benchmarking studies, where they enable consistent comparison of clustering algorithms across datasets with known class structure.

3. Preliminaries

Let $n \in \mathbb{N}$ with $n \geq 4$. We consider a dataset consisting of n objects indexed by the set $\{1, \dots, n\}$. Each pair of objects is associated with a measure of dissimilarity (or distance), and all pairwise dissimilarities are collected in the dataset's dissimilarity matrix.

Definition 1 (Dissimilarity matrix). *A matrix $\Delta \in \mathbb{R}^{n \times n}$ is a dissimilarity matrix if*

- (a) $\Delta_{ij} \geq 0$ for all i, j (Δ is non-negative),
- (b) $\Delta_{ii} = 0$ for all i (Δ has zero diagonal), and
- (c) $\Delta_{ij} = \Delta_{ji}$ for all i, j (Δ is symmetric).

The triangle inequality is not required. We also exclude matrices containing a row of all zeros.

For our purposes, it will be convenient to work with the off-diagonal entries of Δ , sorted row-wise in ascending order. We denote this transformed dissimilarity matrix by $\hat{\Delta}$ ($\hat{\Delta} \in \mathbb{R}^{n \times n-1}$).

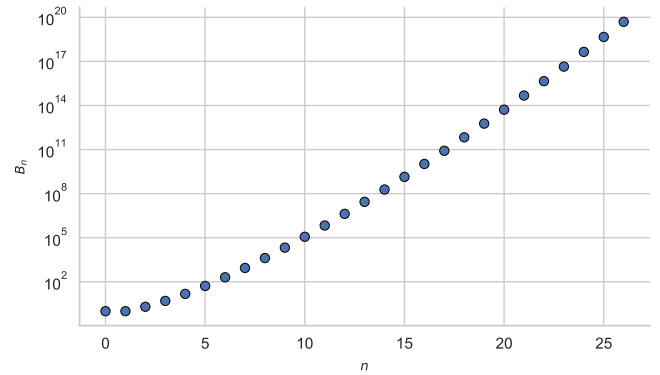


Figure 3: The first 27 Bell numbers, which enumerate the partitions of an n -element set. This rapid growth highlights the combinatorial explosion of clustering possibilities as n increases.

In other words, we have for every i $\{\Delta_{ij}\}_{j=1}^n \setminus \{\Delta_{ii}\} = \{\hat{\Delta}_{ij}\}_{j=1}^{n-1}$ and $\hat{\Delta}_{i1} \leq \hat{\Delta}_{i2} \leq \dots \leq \hat{\Delta}_{i(n-1)}$. Constructing $\hat{\Delta}$ requires sorting each of the n rows of Δ , which costs $O(n^2 \log n)$ time in total.

Now, let us formally define the concept of a clustering of the dataset $\{1, \dots, n\}$.

Definition 2 (Clustering). *Let $K \in \{2, \dots, n\}$. A **K-clustering** of $\{i\}_{i=1}^n$ is a set $C_K = \{C_I\}_{I=1}^K$ such that $C_I \subsetneq \{i\}_{i=1}^n$ for any I , and*

- (a) $\bigcup_{I=1}^K C_I = \{1, \dots, n\}$,
- (b) $C_I \cap C_J = \emptyset$ for $I \neq J$, and
- (c) $C_I \neq \emptyset$ for all $I \in \{1, \dots, K\}$.

The total number of clusterings of an n -element set grows according to the Bell numbers (Fig. 3), illustrating the combinatorial complexity of the clustering problem.

We will now define the silhouette width, which was introduced in 1987 by P.J. Rousseeuw (Rousseeuw, 1987). We employ similar notation.

Definition 3 (Silhouette). *Let C_K be a K -clustering of the dataset $\{1, \dots, n\}$ with dissimilarity matrix Δ . The silhouette width for data point $i \in C_I$ is 0 if $|C_I| = 1$; otherwise it is*

$$s(i|C_K, \Delta) := \frac{b(i) - a(i)}{\max\{a(i), b(i)\}},$$

where

$$a(i) := \frac{1}{|C_I| - 1} \sum_{j \in C_I \setminus \{i\}} \Delta_{ij}, \quad \text{and} \quad b(i) := \min_{J \neq I} \left(\frac{1}{|C_J|} \sum_{j \in C_J} \Delta_{ij} \right).$$

The average silhouette width (ASW) is defined as

$$\text{ASW}(C_K, \Delta) := \frac{1}{n} \sum_{i=1}^n s(i|C_K, \Delta).$$

Note that the silhouette width of i may be written as

$$s(i|C_K, \Delta) = \begin{cases} 1 - a(i)/b(i) & \text{if } a(i) < b(i), \\ 0 & \text{if } a(i) = b(i), \\ b(i)/a(i) - 1 & \text{if } a(i) > b(i). \end{cases}$$

Consequently, $-1 \leq s(i|C_K, \Delta) \leq 1$.

Individual silhouette widths provide a valuable graphical diagnostic, but for large n it is customary to summarize the clustering quality by ASW (Lenssen & Schubert, 2022). A common heuristic is to run a clustering algorithm for several choices of K and select the value that maximizes ASW. When even that maximum is low, it is possible that the limitation stems from the intrinsic structure of the dissimilarity data. This raises the natural question: given a dissimilarity matrix, what is the highest possible ASW? To discuss this question, let C^* denote a silhouette-optimal clustering.

Definition 4 (Silhouette-optimal clustering). *Let Δ be the dissimilarity matrix of the dataset $\{1, \dots, n\}$. We define*

$$\mathfrak{C} := \{C_K : C_K \text{ is a } K\text{-clustering of } \{1, \dots, n\}\}$$

to be the set of all possible clusterings. Any

$$C^* \in \operatorname{argmax}_{C_K \in \mathfrak{C}} \{\text{ASW}(C_K, \Delta)\}$$

is called a **silhouette-optimal clustering**.

4. A data-dependent upper bound of the silhouette

We propose a data-dependent ceiling on the ASW that can be computed before any clustering is performed. For each data point, we derive a sharp upper bound of its silhouette width. Here, *sharp* means that the individual silhouette width of a data point can never exceed the bound, and there exists a clustering in which the bound is exactly achieved. Averaging these per-point ceilings produces a single, dataset-level upper bound on the ASW. The bound is computed from the dissimilarity matrix of the dataset in $O(n^2 \log n)$ time, and the proposed algorithm supports optional minimum cluster size constraints to further tighten the bound.

Consider an arbitrary clustering C_K of the dataset $\{1, \dots, n\}$ with dissimilarities Δ . We will now formalize the upper bound of the silhouette width for point i , i.e. $s(i|C_K, \Delta)$.

For data point i , let $|C_I|$ denote the size of its cluster in C_K . The average distance between i and the remaining data points in the same cluster is not less than the average distance between i and the $|C_I| - 1$ data points closest to i . Similarly, the average distance between i and the $n - |C_I|$ points farthest from i is not smaller than the average distance between i and the data points in the neighboring cluster closest to i . These two observations are combined to construct a value that is guaranteed to be greater than or equal to $s(i|C_K, \Delta)$. We formalize this reasoning through the Λ -quotient of point i .

Definition 5. Let $\Lambda \in \mathbb{N}$ with $1 \leq \Lambda \leq n - 1$. The Λ -quotient of data point i is

$$q(i, \Delta, \Lambda) := \begin{cases} \frac{n - \Lambda}{\Lambda - 1} \cdot \frac{\sum_{j=1}^{\Lambda-1} \hat{\Delta}_{ij}}{\sum_{j=\Lambda}^{n-1} \hat{\Delta}_{ij}} & \text{if } \Lambda > 1, \\ 1, & \text{if } \Lambda = 1. \end{cases}$$

Recall the following basic fact.

Lemma 1. Let $A = \{a_1, \dots, a_N\}$ be a collection of N real values, and consider a partition of A into subsets A_1, \dots, A_M . Then

$$\min_L \frac{1}{|A_L|} \sum_{a \in A_L} a \leq \frac{1}{|A|} \sum_{a \in A} a.$$

Proof. Let $\mu = \frac{1}{|A|} \sum_{a \in A} a$ and $\mu_L = \frac{1}{|A_L|} \sum_{a \in A_L} a$. We have $\mu = \sum_{L=1}^M \frac{|A_L|}{|A|} \mu_L$, and since $\sum |A_L| = |A|$, the statement holds. \square

Proposition 1. Let C_K be a K -clustering of the dataset $\{i\}_{i=1}^n$ with dissimilarities Δ . Let i represent any data point and let $C_I \in C_K$ denote the cluster that contains i . Furthermore, let

$$f(i, \Delta) := \min_{1 \leq \Lambda \leq n-1} \{q(i, \Delta, \Lambda)\}$$

denote a minimal Λ -quotient. Then

$$s(i|C_K, \Delta) \leq 1 - f(i, \Delta).$$

Proof. Suppose $q(i, \Delta, 2) > 1$. Then $(n - 2)\hat{\Delta}_{i1} > \sum_{j=2}^{n-1} \hat{\Delta}_{ij}$, which contradicts $\hat{\Delta}_{i1} \leq \hat{\Delta}_{ij}$ for $j \geq 2$. Hence, $0 \leq f(i, \Delta) \leq 1$. This proves the statement if $|C_I| = 1$ and for cases $a(i) \geq$

$b(i)$ when $|C_I| > 1$. Consider $q(i, \Delta, |C_I|)$. It is clear that $\sum_{j=1}^{|C_I|-1} \hat{\Delta}_{ij}/(|C_I|-1) \leq a(i)$. It remains to argue that $\sum_{j=1}^{n-1} \hat{\Delta}_{ij}/(n-|C_I|) \geq b(i)$. By Lemma 1, we have

$$\begin{aligned} \frac{1}{n-|C_I|} \sum_{j=1}^{n-1} \hat{\Delta}_{ij} &\geq \frac{1}{n-|C_I|} \sum_{j \in \bigcup_{J \neq I} C_J} \Delta_{ij} \\ &\geq \min_{J \neq I} \left(\frac{1}{|C_J|} \sum_{j \in C_J} \Delta_{ij} \right) = b(i). \end{aligned}$$

Thus, $f(i, \Delta) \leq q(i, \Delta, |C_I|) \leq a(i)/b(i)$ and $1 - f(i, \Delta) \geq 1 - a(i)/b(i)$. \square

Taking the mean of all silhouette width upper bounds from Proposition 1 results in the following inequality, which is the main observation of this paper:

$$ASW(C^*, \Delta) \leq 1 - \frac{1}{n} \sum_i f(i, \Delta). \quad (1)$$

We remark that the right-hand side in 1 depends only on the underlying data Δ . Crucially, we note that $1 - \frac{1}{n} \sum_i f(i, \Delta) \leq 1$. Moreover, since any Λ -quotient naturally corresponds to a 2-clustering of the dataset, the bound in Proposition 1 is indeed sharp.

Finally, imposing the narrower definition

$$f_\kappa(i, \Delta) := \min_{\kappa \leq \Lambda \leq n-\kappa} \{q(i, \Delta, \Lambda)\}$$

for some $\kappa \in \{1, \dots, \lfloor n/2 \rfloor\}$ is equivalent to constraining the solution space to clusterings having $\min_I |C_I| \geq \kappa$. Often, as we shall see, this leads to strictly tighter limits.

4.1. Algorithm

The workflow for computing the proposed upper bound is illustrated in Fig.4. Following this workflow, Algo. 1 computes for each data point i the quantity $1 - f_\kappa(i, \Delta)$, which is a sharp upper bound of the silhouette width of i in the solution space $\min_I |C_I| \geq \kappa$. The array A collects these values across all points, and its average equals the dataset-level upper bound.

Time complexity. The formation of $\hat{\Delta}$ requires sorting each of the n rows, which costs $O(n^2 \log n)$. The subsequent linear scans are $O(n^2)$, so the overall run time is $O(n^2 \log n)$. This is slightly slower than computing the ASW, which takes $O(n^2)$ time (Lenssen & Schubert, 2022).

Output summaries. Given Δ and $\kappa = 1$, let $UB(\Delta)$ denote the mean of the output array A from Algo. 1. Then $UB(\Delta)$ corresponds to the right-hand side of Eq. (1). We refer to this as the *global upper bound*. Choosing $\kappa > 1$ imposes the restriction that no cluster is allowed to contain fewer than κ objects. Let $UB_\kappa(\Delta)$ denote the ASW upper bound for this constrained solution space. We will refer to $UB_\kappa(\Delta)$ as an *adjusted upper bound*.

Remark. The upper bound $UB(\Delta)$ is not guaranteed to be close to the true global maximum of ASW. Its tightness is data-dependent.

Algorithm 1: Silhouette upper bound (pointwise)

```

Input:  $\Delta \in \mathbb{R}^{n \times n}$ ; // Dissimilarity matrix
Input:  $\kappa$ ; // Smallest allowed cluster size,
            $1 \leq \kappa \leq \lfloor n/2 \rfloor$ 
Output:  $A \in \mathbb{R}^n$ ; // Array of individual
           upper bounds
1 Initialize array  $A \leftarrow []$ ;
2 Compute  $\hat{\Delta}$  from  $\Delta$ ;
3 for  $i = 1, \dots, n$  do
4    $y \leftarrow \sum_{j=\kappa}^{n-1} \hat{\Delta}_{i,j}$ ;
5    $x \leftarrow 0$ ;
6    $q \leftarrow 1$ ; // Initialize  $\Lambda$ -quotient
7   if  $\kappa > 1$  then
8      $x \leftarrow \sum_{j=1}^{\kappa-1} \hat{\Delta}_{i,j}$ ;
9      $q \leftarrow \frac{x}{\kappa-1} / \frac{y}{n-\kappa}$ ;
10  for  $\Lambda = \kappa + 1, \dots, n - \kappa$  do
11     $x \leftarrow x + \hat{\Delta}_{i,\Lambda-1}$ ;
12     $y \leftarrow y - \hat{\Delta}_{i,\Lambda-1}$ ;
13     $q_{\text{candidate}} \leftarrow \frac{x}{\Lambda-1} / \frac{y}{n-\Lambda}$ ;
14    if  $q_{\text{candidate}} < q$  then
15       $q \leftarrow q_{\text{cand}}$ ; // Update minimal
            $\Lambda$ -quotient
16  Append  $1 - q$  to  $A$ ;
17 return  $A$ 

```

Use cases. In theory, when sharp, the upper bound $UB(\Delta)$ can be used to confirm that an empirical ASW has reached the global optimum. Even when loose, it increases the interpretability of empirical measurements.

In real-world scenarios where the global upper bound appears loose, we speculate that adjusted versions can provide more practical use.

The individual silhouette width upper bounds generated by Algo. 1 provide a neat complement to standard silhouette visualizations, where the point-wise silhouette widths are typically displayed next to each other in a bar graph.

In the Experiments section, we examine these use cases.

4.2. Extension to the macro-averaged silhouette

The standard ASW can produce misleading results when the clusters vary greatly in size. In (Pavlopoulos et al., 2025), John Pavlopoulos, Georgios Vardakas, and Aristidis Likas show that the so-called macro-averaged silhouette is more robust to cluster-size imbalance. For clustering $C_K = \{C_I\}_{I=1}^K$, the macro-averaged silhouette is defined as

$$S_{\text{macro}}(C_K, \Delta) := \frac{1}{K} \sum_{I=1}^K \frac{1}{|C_I|} \sum_{i \in C_I} s(i).$$

In practical scenarios where clusters are imbalanced and small groups also matter, this aggregation strategy is more reasonable. In this subsection, we use Proposition 1 to construct an upper bound for this silhouette variant in a constrained solution space.

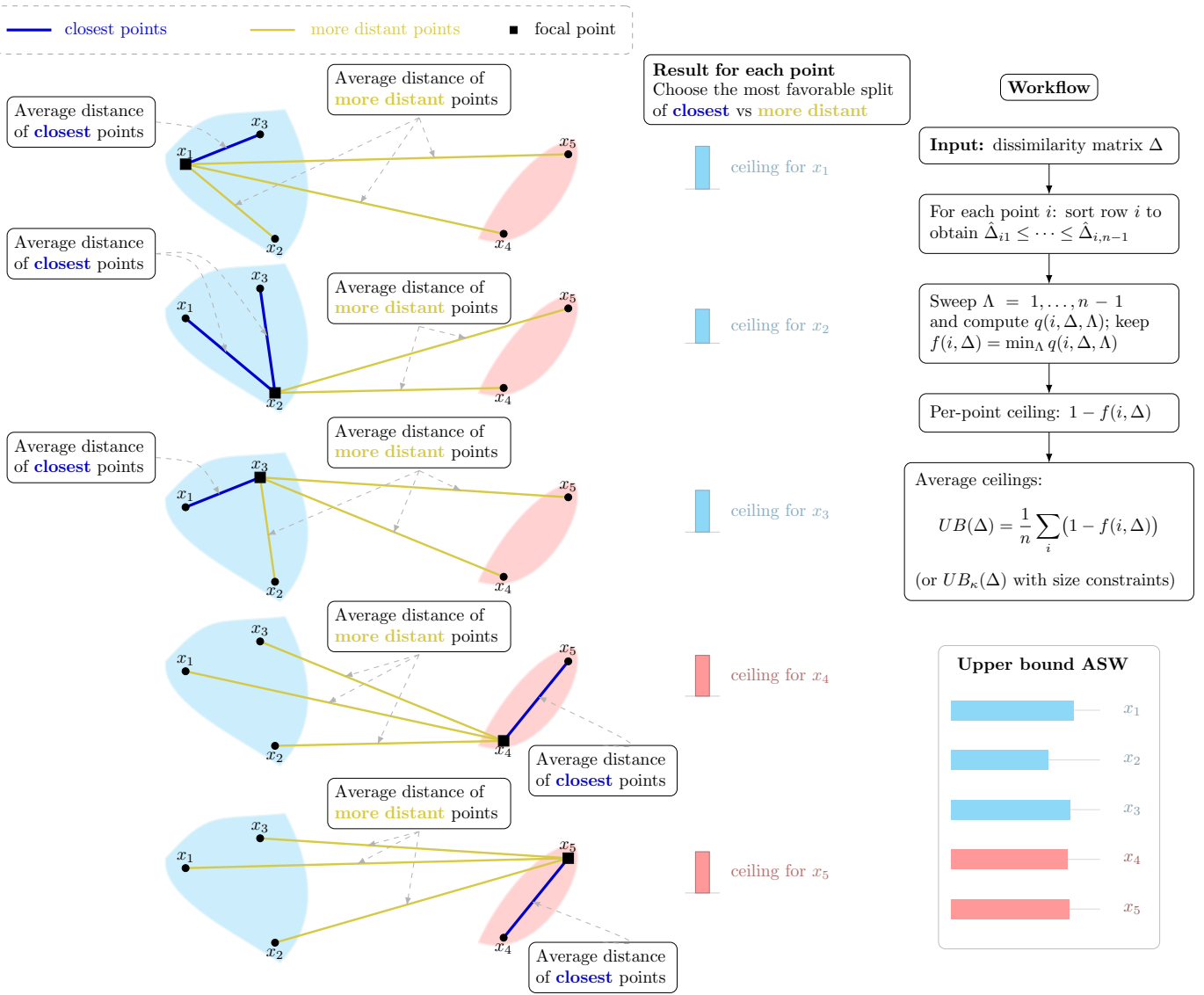


Figure 4: Workflow for computing the proposed ASW upper bound.

Consider an empirical clustering result $\widehat{C}_K = \{\widehat{C}_I\}_{I=1}^K$. We narrow our scope in this context to include all clusterings whose cluster sizes match those of \widehat{C}_K . This narrower solution space is still generally astronomically large. Thus, an efficiently computable data-dependent upper bound is of interest as a relevant benchmark. Let $C_K = \{C_I\}_{I=1}^K$ be any clustering from our constrained solution space, and let ub_i denote the silhouette width upper bound of data point i , i.e. $s(i|C_K, \Delta) \leq ub_i$. Moreover, let $\{ub_{\sigma(i)}\}_{i=1}^n$ denote the upper bounds sorted in ascending order, and let $\{N_I\}_{I=1}^K$ denote the assumed cluster sizes in descending order. With $N_0 := 1$, it follows from the rearrangement inequality that

$$\begin{aligned} S_{macro}(C_K, \Delta) &\leq \frac{1}{K} \sum_{I=1}^K \sum_{i \in C_I} \frac{1}{|C_I|} ub_i \\ &\leq \frac{1}{K} \sum_{I=1}^K \frac{1}{N_I} \sum_{i=\sum_{J=0}^{I-1} N_J}^{\sum_{J=1}^I N_J} ub_{\sigma(i)}. \end{aligned}$$

The last expression is independent of any particular cluster assignment and therefore provides a valid upper bound on the macro-averaged silhouette across all clusterings within the con-

strained solution space. This formulation is particularly useful in applications where cluster sizes are known or can be reasonably estimated. Even in the absence of such assumptions, the resulting bound serves as a sharper and more informative benchmark for evaluating empirical clustering results.

5. Experiments, results & discussion

We evaluate the ASW upper bound by applying it to a variety of datasets, both synthetic and real-world. Multiple distance metrics are considered to examine the behavior of the upper bound under different notions of dissimilarity. The code used for the experiments is available in the GitHub repository <https://github.com/hugo-strang/silhouette-upper-bound>.

An essential part of the evaluation is to establish a nearly tight lower bound for $ASW(C^*, \Delta)$. To this end, we use PAMSIL clustering to obtain an empirical ASW. The closer this value is to the upper bound, the narrower the interval in which the true global maximum lies. PAMSIL is a suitable algorithm since its objective is to maximize ASW.

Given an empirical ASW value, say \widehat{S} , the performance

Table 1: **Real-world datasets.** Datasets used in the experiments and their characteristics. The Metric column indicates the distance metrics used.

Dataset	Title	Instances	Features	Classes	Field	Metric
Ceramic	Chemical Composition of Ceramic Samples	88	17	2	Physics	Manhattan
Customers	Wholesale customers	378	7	2	Business	Cosine
Dermatology	Dermatology	366	34	6	Health and Medicine	Cosine
Heart Statlog	Statlog (Heart)	231	13	2	Health and Medicine	Euclidean
Optdigits	Optical Recognition of Handwritten Digits	2296	64	10	Computer Science	Euclidean
Rna	Gene expression cancer RNA-Seq	808	20531	5	Biology	Euclidean
Wdbc	Wisconsin Diagnostic Breast Cancer	382	30	2	Health and Medicine	Euclidean
Wine	Wine	178	13	3	Chemistry	Manhattan

Table 2: **Experimental results on synthetic data.** Comparison of clustering performance and the proposed upper bound.

Dataset	K	ASW	$UB(\Delta)$	Worst-case rel. error
400-64-5-6	5	0.249	0.376	0.339
400-64-2-2	2	0.673	0.673	0.000
400-128-7-3	7	0.522	0.566	0.078
1000-300-5-2	5	0.668	0.678	0.015
10000-32-20-2	20	0.626	0.774	0.192
10000-1024-20-4	20	0.417	0.454	0.081

metric of interest is the *relative error*, defined as

$$\frac{\text{ASW}(C^*, \Delta) - \widehat{S}}{\text{ASW}(C^*, \Delta)},$$

where C^* denotes a clustering that achieves the global maximum. Since $\text{ASW}(C^*, \Delta)$ is unknown in practice, we use the global upper bound $UB(\Delta)$ to obtain a conservative estimate:

$$\frac{\text{ASW}(C^*, \Delta) - \widehat{S}}{\text{ASW}(C^*, \Delta)} \leq \frac{UB(\Delta) - \widehat{S}}{UB(\Delta)}.$$

We refer to this quantity as the *worst-case relative error*. Its interpretation is straightforward: if the worst-case relative error falls below a tolerance ϵ , then the empirical ASW is guaranteed to be within ϵ of the true maximum.

Synthetic datasets. We follow (de Amorim & Makarenkov, 2025) in notation and approach. Synthetic datasets are generated using the `make_blobs` function from `scikit-learn` (Pedregosa et al., 2012). Each dataset is labeled as $n_samples - n_features - centers - cluster_std$, indicating the parameter values used to generate the points. For example, 400-16-3-4 denotes a dataset of 400 16-dimensional vectors partitioned into 3 clusters with standard deviation 4, which controls within-cluster dispersion. Finally, for these datasets, we use Euclidean distance.

Real-world datasets. We evaluate our method on eight real-world datasets from the UCI Machine Learning Repository (Kelly

et al.), commonly used in clustering and classification research. Table 1 summarizes their key characteristics along with the distance metrics employed. Standard preprocessing steps, including feature scaling and outlier removal, are applied where appropriate. Each dataset provides a known number of classes, which we use to determine the number of clusters K . When all class labels are available, we report the ARI and AMI to verify that these datasets represent meaningful clustering structures. In that way, we ensure that our experiments are conducted in natural clustering contexts.

Results. In Table 2, we apply the upper bound to six synthetic datasets and compare the results with PAMSIL clustering. For dataset 400-64-2-2, the upper bound at 0.673 confirms that PAMSIL reaches a globally optimal silhouette score. For three of the remaining datasets, $UB(\Delta)$ proves that the PAMSIL ASW is within 8 % of the global maximum, that is, essentially optimal. For dataset 400-64-5-6 with $UB(\Delta) = 0.376$, we record an empirical ASW of 0.249. In this case, it remains unclear whether further substantial improvements of the ASW are possible. However, interpreting the attained value in the interval $[-1, 0.376]$ enables more well-founded conclusions compared to using the standard range $[-1, 1]$.

Table 3 examines the performance of PAMSIL on the eight real-world datasets and compares it with the upper bounds. In these cases, the global upper bounds provide information that is less actionable. It is unclear whether the reason for this is that the attained ASW values are far from $\text{ASW}(C^*, \Delta)$, or that

Table 3: **Experimental results on real data.** Comparison of clustering performance and the proposed upper bound.

Performance of PAMSIL clustering					Comparison with global upper bound		Comparison with adjusted upper bound		
Dataset	K	$\min_I\{ C_I \}$	ARI	AMI	ASW	$UB(\Delta)$	Worst-case rel. error	$UB_K(\Delta)$	Worst-case rel. error
Ceramic	2	44	1.000	1.000	0.358	0.621	0.423	0.403	0.112
Customers	2	170	0.394	0.366	0.400	0.951	0.579	0.574	0.303
Dermatology	6	21	0.850	0.875	0.455	0.836	0.456	0.704	0.354
Heart Statlog	2	83	0.447	0.349	0.161	0.600	0.731	0.279	0.422
Optdigits	10	50	0.803	0.819	0.180	0.620	0.709	0.463	0.611
Rna	5	77	—	—	0.225	0.419	0.464	0.323	0.303
Wdbc	2	46	0.427	0.386	0.348	0.621	0.440	0.455	0.236
Wine	3	53	0.884	0.864	0.315	0.649	0.514	0.450	0.298

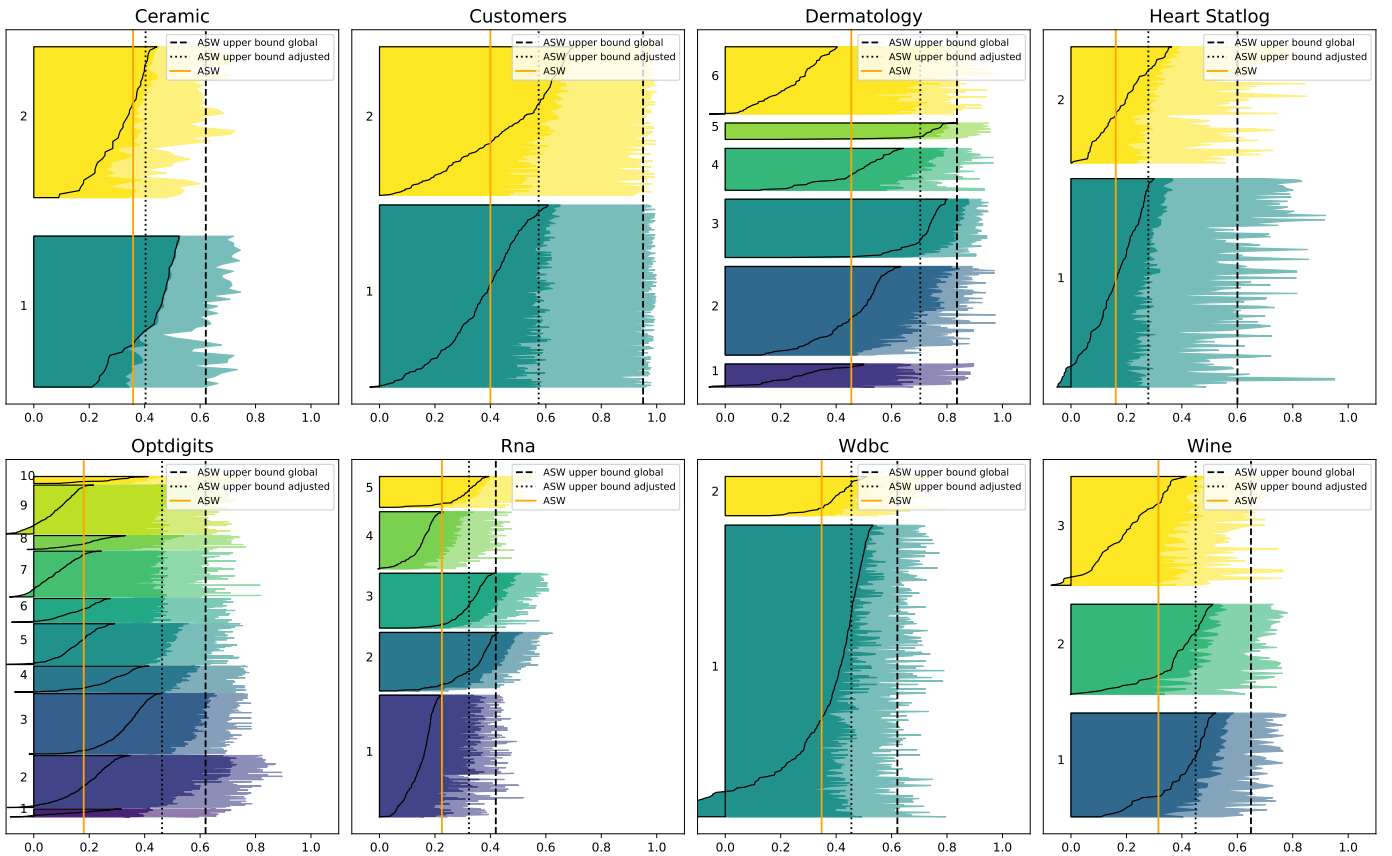


Figure 5: Silhouette plots for the eight real-world datasets. PAMSIL clustering with K equal to the ground truth number of classes; ASW compared against the global upper $UB(\Delta)$ and the adjusted upper bound $UB_K(\Delta)$, with κ being the smallest cluster size. The solid contour lines indicate the point-wise silhouette widths, the opaque areas indicate the corresponding adjusted upper bounds, while the transparent areas indicate the corresponding global upper bounds.

the upper bounds are somewhat loose, or both. However, the adjusted upper bounds $UB_K(\Delta)$ are considerably tighter for most datasets. Here, κ is set to the minimum cluster size in the PAMSIL solution. For datasets Ceramic, Customers, Rna, Wdbc and Wine, $UB_K(\Delta)$ proves that the ASW-values attained by PAMSIL are within 30 % of the corresponding optimums.

Fig. 5 shows classical silhouette visualizations corresponding to the PAMSIL clusters, complemented with upper bounds of the individual silhouette widths. The solid contour lines indicate

the point-wise silhouette widths, the opaque areas indicate the corresponding adjusted upper bounds, while the transparent areas indicate the corresponding global upper bounds. For the adjusted upper bounds, κ is set to the smallest cluster size in the generated solution. This method provides a visual comparison of the empirical silhouette and the highest possible value at the data point level.

In Fig. 6 we show, for each real-world dataset and for each $K \in \{2, \dots, 15\}$, the attained ASW value compared to the global

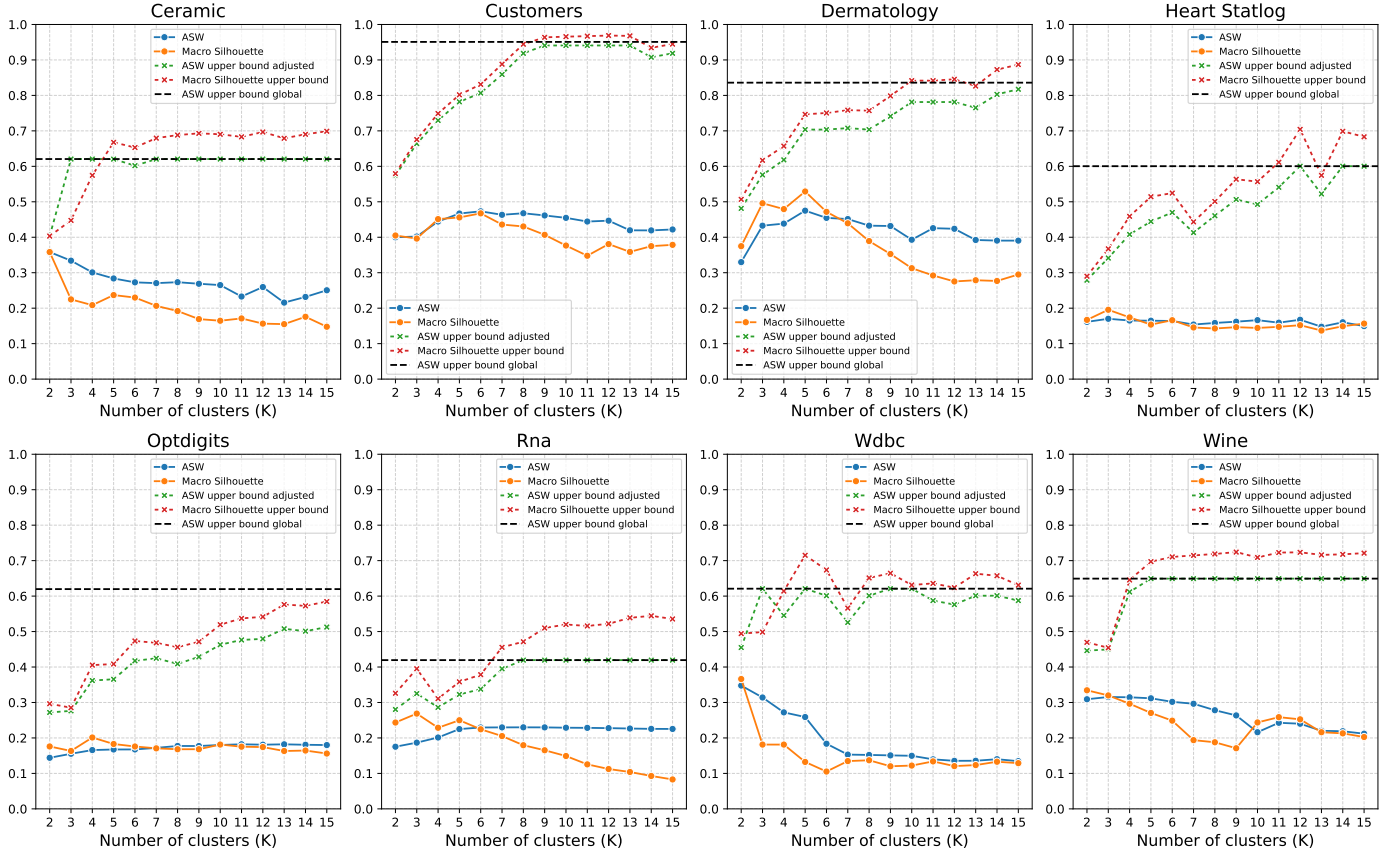


Figure 6: PAMSIL performance for varying K and comparison with upper bounds.

ASW upper bound. Additionally, at each K , we compare the ASW to the adjusted upper bound $UB_k(\Delta)$ with κ set to the minimum cluster size in the corresponding solution. Lastly, we include, at each K , the recorded macro-averaged silhouette and compare this value with the upper bound derived in Section 4.2.

Discussion. We summarize with some reflections on the practical relevance of the proposed upper bound.

Replacing the standard ASW range $[-1, 1]$ with the data-dependent interval $[-1, UB(\Delta)]$ enhances the interpretability of observed ASW values. However, when the empirical ASW lies far below the upper bound, it remains unclear whether further improvement is actually possible. We suspect that this gap often persists for the global upper bound, even when the empirical ASW is close to $ASW(C^*, \Delta)$. In many real-world applications, however, analysts impose minimum cluster-size constraints to avoid overly small or degenerate clusters. By incorporating such constraints through κ , the refined bound $UB_k(\Delta)$ better reflects the relevant solution space and provides more meaningful guidance in practice. As demonstrated in Table 3, $UB_k(\Delta)$ ensures that the PAMSIL solutions are within 30 % of the optimum for five of the examined datasets, indicating strong empirical performance under realistic conditions. In such cases, the bound can be used to conclude that further exploration would, at best, yield only marginally better results.

6. Conclusion

In this paper, we proposed a dataset-dependent upper bound on the average silhouette width ASW as a complementary tool for analyzing clustering quality. While ASW is conventionally interpreted relative to its standard range $[-1, 1]$, our results show that a tighter data-dependent upper bound can be computed in $O(n^2 \log n)$ time. This upper bound provides a more meaningful reference value. It often lies well below 1, reflecting the inherent limitations of the dataset itself.

Empirical studies on both synthetic and real datasets confirm that the proposed upper bound is often nearly tight and yields valuable insights into the structure and limitations of the data. At the same time, we emphasize that the bound is not guaranteed to be sharp in general; the true global ASW-maximum may fall considerably below the bound. For this reason, the bound should not be viewed as a precise target but as an informative ceiling that frames observed ASW scores in a sharper context.

From a broader perspective, our main contribution is to establish a proof of concept: that efficiently computable, data-dependent upper bounds on ASW can enrich cluster analysis. We believe this idea opens a promising direction for future work, where the focus should be on deriving tighter bounds and extending the framework to other internal clustering validity indices. An important next step is to better understand under which conditions the proposed bound is most informative in practice — for instance, how its tightness varies with properties of the data,

the dissimilarity metric, the dimensionality of the feature space, or the number of underlying clusters. Such insights would clarify in which contexts the bound provides the greatest practical value.

Declaration of competing interest

The authors declare that they have no known competing financial interests or personal relationships that could have appeared to influence the work reported in this paper.

CRediT authorship contribution statement

Hugo Sträng: conceptualization, data curation, methodology, experiment, visualization, writing, editing; Tai Dinh: visualization, writing, editing, validation.

Acknowledgments

The authors would like to thank Hugo Fernström for his careful proofreading and thoughtful feedback on an earlier version of this manuscript. His continuous encouragement has been greatly appreciated throughout the development of this work.

We are also grateful to several researchers for their valuable comments and suggestions on a previous version of the paper.

References

Aggarwal, C. C. (2013). An introduction to cluster analysis. In *Data Clustering: Algorithms and Applications* (pp. 1–28). Chapman and Hall/CRC.

Alrasheed, M., & Mourshed, M. (2024). Building stock modelling using k-prototype: A framework for representative archetype development. *Energy and Buildings*, 311, 114111.

de Amorim, R. C., & Makarenkov, V. (2025). Improving clustering quality evaluation in noisy gaussian mixtures. [arXiv:2503.00379](https://arxiv.org/abs/2503.00379).

Ansari, M. Y., Mainuddin, Ahmad, A., & Bhushan, G. (2021). Spatiotemporal trajectory clustering: A clustering algorithm for spatiotemporal data. *Expert Systems with Applications*, 178, 115048.

Aonso-Diego, G., Macía, L., Montero, M., & Estévez, A. (2024). Cluster analysis based on gambling variables and mental health in a clinical population of gamblers. *Addictive Behaviors*, 157, 108092.

Bagirov, A., Hoseini-Monjezi, N., & Taheri, S. (2023a). A novel optimization approach towards improving separability of clusters. *Computers & Operations Research*, 152, 106135.

Bagirov, A. M., Aliguliyev, R. M., & Sultanova, N. (2023b). Finding compact and well-separated clusters: Clustering using silhouette coefficients. *Pattern Recognition*, 135, 109144.

Bai, X., Xie, Z., Xu, X., & Xiao, Y. (2023). An adaptive threshold fast DBSCAN algorithm with preserved trajectory feature points for vessel trajectory clustering. *Ocean Engineering*, 280, 114930.

Baier, P. C., Sahlström, H., Markström, A., Furmark, T., & Bothelius, K. (2024). Nocturnal sleep phenotypes in idiopathic hypersomnia – A data-driven cluster analysis. *Sleep Medicine*, 124, 127–133.

Balbi, E., Cianfarra, P., Crispini, L., Tosi, S., & Ferretti, G. (2024). Hierarchical-agglomerative clustering analysis of geomorphic features applied to tectonic investigation of terrestrial planets: An example from Claritas Fossae, Mars. *Icarus*, 420, 116197.

Batool, F., & Hennig, C. (2021). Clustering with the Average Silhouette Width. *Computational Statistics & Data Analysis*, 158, 107190.

Bhagat, H. V., & Singh, M. (2022). Dpcf: A framework for imputing missing values and clustering data in drug discovery process. *Chemometrics and Intelligent Laboratory Systems*, 231, 104686.

Bi, M., Chen, H., & Zuo, M. (2025). Comprehensive quality grading and dynamic prediction of physicochemical indicators of maize during storage based on clustering and time-series prediction models. *Journal of Cereal Science*, 123, 104187.

Biabiany, E., Bernard, D. C., Page, V., & Paugam-Moisy, H. (2020). Design of an expert distance metric for climate clustering: The case of rainfall in the Lesser Antilles. *Computers & Geosciences*, 145, 104612.

Caliński, T., & Harabasz, J. (1974). A dendrite method for cluster analysis. *Communications in Statistics*, 3, 1–27.

Capó, M., Pérez, A., & Lozano, J. A. (2023). Fast computation of cluster validity measures for bregman divergences and benefits. *Pattern Recognition Letters*, 170, 100–105.

Chander, S., Vijaya, P., Fernandes, R., Rodrigues, A. P., & R, M. (2023). Dolphin-political optimized tversky index based feature selection in spark architecture for clustering big data. *Advances in Engineering Software*, 176, 103331.

Consuegra-Jiménez, S., Tovio-Gracia, C., Vivas-Reyes, R., & Vivas, R. (2025). Unsupervised learning techniques for clustering analysis of physicochemical properties in the periodic table elements.

Davies, D. L., & Bouldin, D. W. (1979). A cluster separation measure. *IEEE Transactions on Pattern Analysis and Machine Intelligence, PAMI-1*, 224–227.

Deng, S., Tang, H., & Bai, S. (2025). On estimation and order selection for multivariate extremes via clustering. *Journal of Multivariate Analysis*, 208, 105426.

Díaz González, C. A., Mendez Calderón, Y. M., Mojica Cruz, N. A., & Pacheco Sandoval, L. E. (2022). Typologies of Colombian off-grid localities using PCA and clustering analysis for a better understanding of their situation to meet SDG-7. *Cleaner Energy Systems*, 3, 100023.

Dinh, D.-T., Fujinami, T., & Huynh, V.-N. (2019). Estimating the optimal number of clusters in categorical data clustering by silhouette coefficient. In *International Symposium on Knowledge and Systems Sciences* (pp. 1–17). Springer.

Dinh, T., Wong, H., Lisik, D., Koren, M., Tran, D., Yu, P. S., & Torres-Sospedra, J. (2025). Data clustering: a fundamental method in data science and management. *Data Science and Management*, .

Du, P., Li, F., & Shao, J. (2024). Multi-agent reinforcement learning clustering algorithm based on silhouette coefficient. *Neurocomputing*, 596, 127901.

Duarte, J., Vieira, L. W., Marques, A. D., Schneider, P. S., Pumi, G., & Prass, T. S. (2021). Increasing power plant efficiency with clustering methods and Variable Importance Index assessment. *Energy and AI*, 5, 100084.

Dwivedi, R., Tiwari, A., Bharill, N., Ratnaparkhe, M., Singh, S. K., & Tripathi, A. (2025). A novel chemical property-based, alignment-free scalable feature extraction method for genomic data clustering. *Computers and Electrical Engineering*, 123, 110175.

Edris, M., Ghasemi-Varnamkhasti, M., Kiani, S., Yazdanpanah, H., & Izadi, Z. (2024). Identifying the authenticity and geographical origin of rice by analyzing hyperspectral images using unsupervised clustering algorithms. *Journal of Food Composition and Analysis*, 125, 105737.

Enriquez-Loja, J., Castillo-Pérez, B., Serrano-Guerrero, X., & Barragán-Escandón, A. (2025). Performance evaluation method for different clustering techniques. *Computers and Electrical Engineering*, 123, 110132.

Eskandarnia, E., Al-Ammal, H. M., & Ksantini, R. (2022). An embedded deep-clustering-based load profiling framework. *Sustainable Cities and Society*, 78, 103618.

Fu, N., Ni, W., Zhang, S., Hou, L., & Zhang, D. (2023). Gc-NLDP: A graph clustering algorithm with local differential privacy. *Computers & Security*, 124, 102967.

Fu, Y.-G., Chen, X., Xu, S., Li, J., Yao, X., Huang, Z., & Wang, Y.-M. (2025). Gsscl: A framework for Graph Self-Supervised Curriculum Learning based on clustering label smoothing. *Neural Networks*, 181, 106787.

Gagolewski, M., Bartoszuk, M., & Cena, A. (2021). Are cluster validity measures (in) valid? *Information Sciences*, 581, 620–636.

Gan, H., Gan, W., Yang, Z., & Zhou, R. (2024). Discrimination-aware safe semi-supervised clustering. *Information Sciences*, 676, 120798.

Gere, A. (2023). Recommendations for validating hierarchical clustering in consumer sensory projects. *Current Research in Food Science*, 6, 100522.

Ghaderi, H., Foreman, B., Nayebi, A., Tipirneni, S., Reddy, C. K., & Subbian, V. (2023). A self-supervised learning-based approach to clustering multivariate time-series data with missing values (SLAC-Time): An application to TBI phenotyping. *Journal of Biomedical Informatics*, 143, 104401.

Gill, E. R., Dill, C., Goss, C. H., Sagel, S. D., Wright, M. L., Horner, S. D., & Zuñiga, J. A. (2024). Symptom phenotyping in people with cystic fibrosis during acute pulmonary exacerbations using machine-learning K-means clustering analysis. *Journal of Cystic Fibrosis*, 23, 1106–1111.

Guan, Y., Lu, H., Dong, J., Ge, Y., Zhang, W., & Deng, Y. (2025). A novel groundwater pollution risk assessment method for producing-enterprises sites: Integrating scenario-specific pollution evaluation with Gaussian mixture model clustering. *Process Safety and Environmental Protection*, 195, 106760.

Gulma, U. L. (2022). A new geodemographic classification of the influence of neighbourhood characteristics on crime: The case of Leeds, UK. *Computers, Environment and Urban Systems*, 92, 101748.

Guo, X., Fang, M., Tang, L., Kan, Z., Yang, X., Pei, T., Li, Q., & Li, C. (2025). An adaptive OD flow clustering method to identify heterogeneous urban mobility trends. *Journal of Transport Geography*, 123, 104080.

Guo, X., Yang, Z., Li, C., Xiong, H., & Ma, C. (2023). Combining the classic vulnerability index and affinity propagation clustering algorithm to assess the intrinsic aquifer vulnerability of coastal aquifers on an integrated scale. *Environmental Research*, 217, 114877.

Gupta, R., Mathur, J., & Garg, V. (2025). A criteria-based climate classification approach considering clustering and building thermal performance: Case of India. *Building and Environment*, 270, 112512.

Hu, H., Zhao, J., Bian, X., & Xuan, Y. (2023). Transformer-customer relationship identification for low-voltage distribution networks based on joint optimization of voltage silhouette coefficient and power loss coefficient. *Electric Power Systems Research*, 216, 109070.

Huang, S., Wu, S., Zhang, H., Wang, J., Song, X., Shen, Y., & Han, L. (2023). Dominant Partitioning of Rock Masses Discontinuities Based on Information Entropy Selective Heterogeneous Ensemble. *KSCE Journal of Civil Engineering*, 27, 5149–5162.

Hubert, L., & Arabie, P. (1985). Comparing partitions. *J. of Classification*, 2, 193–218.

Jain, A. K., Murty, M. N., & Flynn, P. J. (1999). Data clustering: a review. *ACM computing surveys (CSUR)*, 31, 264–323.

Jamalpour, Z., Ghaderi, S., & Fathian-Kolahkaj, M. (2025). High-risk patient profiles for ovarian cancer: A new approach using cluster analysis of tumor markers. *Journal of Gynecology Obstetrics and Human Reproduction*, 54, 102888.

Jha, P., Tiwari, A., Bharill, N., Ratnaparkhe, M., Mounika, M., & Nagendra, N. (2021). Apache Spark based kernelized fuzzy clustering framework for single nucleotide polymorphism sequence analysis. *Computational Biology and Chemistry*, 92, 107454.

Kaufman, L., & Rousseeuw, P. (1990). *Finding Groups in Data: An Introduction To Cluster Analysis*.

Kelly, M., Longjohn, R., & Nottingham, K. (2025). The uci machine learning repository. <https://archive.ics.uci.edu>.

Khan, I. K., Daud, H., Zainuddin, N., & Sokkalingam, R. (2025a). Standardizing reference data in gap statistic for selection optimal number of cluster in K-means algorithm. *Alexandria Engineering Journal*, 118, 246–260.

Khan, I. K., Daud, H. B., Zainuddin, N. B., Sokkalingam, R., Naheed, N., Janisar, A. A., Inayat, A., & Rana, M. S. (2025b). Standardization of expected value in gap statistic using Gaussian distribution for optimal number of clusters selection in K-means. *Egyptian Informatics Journal*, 30, 100701.

Kim, H., Kim, Y.-H., Kim, S.-J., & Choi, M.-T. (2022). Pathological gait clustering in post-stroke patients using motion capture data. *Gait & Posture*, 94, 210–216.

Koren, M., Peretz, O., & Koren, O. (2025). A preprocessing data-driven pipeline for estimating number of clusters. *Engineering Applications of Artificial Intelligence*, 141, 109893.

Kotary, D. K., & Nanda, S. J. (2020). Distributed robust data clustering in wireless sensor networks using diffusion moth flame optimization. *Engineering Applications of Artificial Intelligence*, 87, 103342.

Kotary, D. K., Nanda, S. J., & Gupta, R. (2021). A many-objective whale optimization algorithm to perform robust distributed clustering in wireless sensor network. *Applied Soft Computing*, 110, 107650.

Koutsandreas, D., & Keppo, I. (2024). Harnessing machine learning algorithms to unveil energy efficiency investment archetypes. *Energy Reports*, 12, 3180–3195.

Van der Laan, M., Pollard, K., & Bryan, J. (2003). A new partitioning around medoids algorithm. *Journal of Statistical Computation and Simulation*, .

Lasek, P., Rzasa, W., & Król, A. (2024). Employing Aggregations of Fuzzy Equivalences in Clustering and Visualization of Medical Data Sets. *Procedia Computer Science*, 246, 2733–2742.

Lenssen, L., & Schubert, E. (2022). Clustering by direct optimization of the medoid silhouette. In *Similarity Search and Applications*. Springer International Publishing.

Lenssen, L., & Schubert, E. (2024). Medoid Silhouette clustering with automatic cluster number selection. *Information Systems*, 120, 102290.

Li, P., Dong, Q., Zhao, X., Lu, C., Hu, M., Yan, X., & Dong, C. (2025). Clustering of freeway cut-in scenarios for automated vehicle development considering data dimensionality and imbalance. *Accident Analysis & Prevention*, 220, 108151.

Ma, Y., Schmöcker, J.-D., Sun, W., & Nakao, S. (2025). Unravelling route choices of large trucks using trajectory clustering and conditional Logit models. *International Journal of Transportation Science and Technology*, 17, 238–250.

Manochandar, S., Punniyamoorthy, M., & Jeyachitra, R. (2020). Development of new seed with modified validity measures for k-means clustering. *Computers & Industrial Engineering*, 141, 106290.

Mohd, A., Teoh, L. E., & Khoo, H. L. (2024). Passengers' requests clustering with k-prototype algorithm for the first-mile and last-mile (FMLM) shared-ride taxi service. *Multimodal Transportation*, 3, 100132.

Nourani, V., Ghanei, P., & Kantoush, S. A. (2022). Robust clustering for assessing the spatiotemporal variability of groundwater quantity and quality. *Journal of Hydrology*, 604, 127272.

Ouyang, J., Chu, L., Chen, X., Zhao, Y., Zhu, X., & Liu, T. (2024). A K-means cluster division of regional photovoltaic power stations considering the consistency of photovoltaic output. *Sustainable Energy, Grids and Networks*, 40, 101573.

Owoo, N., & Odei-Mensah, J. (2025). Hierarchical clustering-based early warning model for predicting bank failures: Insights from Ghana's financial sector reforms (2017–2019). *Research in International Business and Finance*, 77, 102944.

Panwar, A., & Nanda, S. J. (2024). Distributed enhanced multi-objective evolutionary algorithm based on decomposition for cluster analysis in wireless sensor network. *Journal of Network and Computer Applications*, 232, 104032.

Panwar, A., & Nanda, S. J. (2025). Distributed robust multitask clustering in wireless sensor networks using Multi-Factorial Evolutionary Algorithm. *Journal of Parallel and Distributed Computing*, 198, 105038.

Passarella, R., Noor, T. M., Arsalan, O., & Adenan, M. S. (2024). Anomaly detection in commercial aircraft landing at SSK II airport using clustering method. *Aerospace Traffic and Safety*, 1, 141–154.

Pavlopoulos, J., Vardakas, G., & Likas, A. (2025). Revisiting silhouette aggregation. In *Discovery Science* (pp. 354–368). Cham: Springer Nature Switzerland.

Pedregosa, F., Varoquaux, G., Gramfort, A., Michel, V., Thirion, B., Grisel, O., Blondel, M., Prettenhofer, P., Weiss, R., Dubourg, V., Vanderplas, J., Passos, A., Cournapeau, D.,

Brucher, M., Perrot, M., Duchesnay, E., & Louppe, G. (2012). Scikit-learn: Machine learning in python. *Journal of Machine Learning Research*, 12.

Pham, D. T., Mai, L. T., & Nguyen, H. V. (2025). Clustering analysis to identify structural and density heterogeneity in Mg₂SiO₄ glass. *Computational Materials Science*, 257, 114019.

Qaroush, A. M., Jubran, M., Olayyan, Q., & Qutait, O. (2025). Maximum relevant diversity aware, multi-video summarization using clustering and evolutionally multi-objective optimization. *Expert Systems with Applications*, 292, 128631.

Qin, J., Sun, X., Du, S., & Ye, J. (2025). A single-valued neutrosophic affinity propagation approach for engineering geological zoning of open-pit mine slopes. *Engineering Applications of Artificial Intelligence*, 146, 110316.

Quintero, Y., Ardila, D., Aguilar, J., & Cortes, S. (2022). Analysis of the socioeconomic impact due to COVID-19 using a deep clustering approach. *Applied Soft Computing*, 129, 109606.

Rodríguez-Gómez, F., del Campo-Ávila, J., & Mora-López, L. (2024). A novel clustering based method for characterizing household electricity consumption profiles. *Engineering Applications of Artificial Intelligence*, 129, 107653.

Rousseeuw, P. J. (1987). Silhouettes: A graphical aid to the interpretation and validation of cluster analysis. *Journal of Computational and Applied Mathematics*, 20, 53–65.

Rustum, Gunawan, A. Y., & Kresnowati, M. T. A. P. (2022). Data dimensionality reduction technique for clustering problem of metabolomics data. *Heliyon*, 8, e09715.

Sancho, A., Ribeiro, J., Reis, M., & Martins, F. (2022). Cluster analysis of crude oils with k-means based on their physico-chemical properties. *Computers & Chemical Engineering*, 157, 107633.

Schubert, E., & Lenssen, L. (2022). Fast k-medoids clustering in rust and python. *Journal of Open Source Software*, 7, 4183.

Sharafoddini, A., Dubin, J. A., & Lee, J. (2021). Identifying subpopulations of septic patients: A temporal data-driven approach. *Computers in Biology and Medicine*, 130, 104182.

Sheng, H., Huang, Z., Ke, L., Zhang, J., Zeng, Z., Yasir, M., & Liu, S. (2025). Multi-scale vessel trajectory clustering: An adaptive DBSCAN method for maritime areas of diverse extents. *Ocean Engineering*, 334, 121461.

Silva-Muñoz, M., Oyarzún, J., Semaan, G., Contreras-Bolton, C., Rey, C., & Parada, V. (2025). Automatic clustering by automatically generated algorithms. *Engineering Applications of Artificial Intelligence*, 159, 111596.

Singh, S., & Gaur, S. (2025). Development and Kohonen neural network based cluster analysis of red rice cookies enriched with blends of different edible seeds flour. *Food Chemistry*, 474, 143127.

Song, W., Wang, Y., & Pan, Z. (2023). A novel cell partition method by introducing Silhouette Coefficient for fast approximate nearest neighbor search. *Information Sciences*, 642, 119216.

Thirumoorthy, K., & Muneeswaran, K. (2021). A hybrid approach for text document clustering using Jaya optimization algorithm. *Expert Systems with Applications*, 178, 115040.

Vinh, N., Epps, J., & Bailey, J. (2009). Information theoretic measures for clusterings comparison: Is a correction for chance necessary? (p. 135).

Waidyanatha, N., & Zuri Sha'ameri, A. (2023). Regularity bounded sensor clustering. *Measurement*, 214, 112810.

Wang, L., Wang, S., Yuan, Z., & Peng, L. (2021). Analyzing potential tourist behavior using PCA and modified affinity propagation clustering based on Baidu index: taking Beijing city as an example. *Data Science and Management*, 2, 12–19.

Xian, Z., & Liu, C. (2025). A systematic framework enhancing molecular screening efficiency in drug discovery via scaffold-driven fuzzy similarity and adaptive spectral clustering. *Computational Biology and Chemistry*, 119, 108559.

Yang, D., Wang, J., He, J., & Zhao, C. (2024). A clustering mining method for sports behavior characteristics of athletes based on the ant colony optimization. *Heliyon*, 10, e33297.

Yang, Q., Yin, J., Liu, M., & Law, S.-s. (2022). A zoning method for the extreme wind pressure coefficients of buildings based on weighted K-means clustering. *Journal of Wind Engineering and Industrial Aerodynamics*, 228, 105124.

Zhang, J., Zhang, J., Liu, H., & Liang, Z. (2025). A two-stage adaptive affinity propagation clustering using the wtDTW distance: Application in portfolio optimization. *Expert Systems with Applications*, 274, 126884.

Zhao, M., Wan, J., & Peng, C. (2023a). Generalized predictive control using improved recurrent fuzzy neural network for a boiler-turbine unit. *Engineering Applications of Artificial Intelligence*, 121, 106053.

Zhao, W., Ma, J., Liu, Q., Song, J., Tysklind, M., Liu, C., Wang, D., Qu, Y., Wu, Y., & Wu, F. (2023b). Comparison and application of SOFM, fuzzy c-means and k-means clustering algorithms for natural soil environment regionalization in China. *Environmental Research*, 216, 114519.

Zheng, R., & Lei, L. (2025). A practical data-driven sampling framework combining KMKFC clustering and MCFS feature selection for large-scale building energy efficiency analysis. *Journal of Building Engineering*, 109, 113043.

Zhou, J., & He, Y. (2025). Recognition of household electricity consumption pattern in smart grid. *Journal of Building Engineering*, 105, 112467.

Zhou, M., Kong, W., Hu, F., Zhu, Z., Wu, C., Wang, L., Zhang, Q., & Zhou, G. (2024). Ocae-based feature extraction and cluster analysis of high-energy-consuming plant loads. *Computers and Electrical Engineering*, 119, 109579.